

Anion Binding of Inorganic Phosphates by the Hexaaza Macrocyclic Ligand 3,6,9,17,20,23-Hexaazatricyclo[23.3.1.1^{11,15}]triaconta-1(29),11(30),12,14,25,27-hexaene

David A. Nation, Joseph Reibenspies, and Arthur E. Martell*

Department of Chemistry, Texas A&M University, College Station, Texas 77843-3255

Received October 12, 1995[Ⓞ]

The interaction of mono-, di-, and triphosphosphate anions with the various protonated forms of the hexaaza macrocyclic ligand BMXD, 3,6,9,17,20,23-hexaazatricyclo[23.3.1.1^{11,15}]triaconta-1(29),11(30),12,14,25,27-hexaene, was investigated by potentiometric equilibrium studies. The protonated ligand forms a number of stable binary complexes in solution with each of the anionic substrates and the strength of interaction increases in the order mono- < di- < triphosphosphate. Formation constants for all the species found are reported and compared with those of analogous systems. The hexahydrobromide salt of BMXD, (H₆BMXD)Br₆·7H₂O crystallizes in the orthorhombic system, space group *Pna*2₁, with *a* = 11.597(4) Å, *b* = 12.604(4) Å, *c* = 27.361(7) Å, and *Z* = 4. The binary complex (H₄BMXD-H₂P₂O₇)Br₂·5.2H₂O crystallizes in the monoclinic system, space group *C2/c*, with *a* = 28.194(6) Å, *b* = 13.875(3) Å, *c* = 20.811(4) Å, *β* = 113.72(3)°, and *Z* = 8. The X-ray structure results reveal the nature of the interaction between the protonated macrocycle and anionic substrates to be that of multiple hydrogen bonding.

Introduction

The binding of organic and inorganic substrates to polyammonium macrocycles and the ensuing chemical reactions of the complexes that result is an area of intense research interest.^{1–3} In particular the interaction of inorganic polyphosphates with these macrocycles is of obvious relevance in view of the enzymatic processes that involve the nucleotide adenosine triphosphate (ATP) and its di- and monophosphate analogs (ADP and AMP respectively). Studies have shown that the hexaaza macrocycle O-BISDIEN is able to form very stable complexes with ATP⁴ and also to catalyze the hydrolysis of ATP to ADP and monophosphate.⁵ In addition this macrocycle was able to effect the phosphorylation of a number of substrates, including ADP, via the formation of a reactive phosphoramidate intermediate.⁶

Successful catalysis by polyammonium macrocycles relies heavily on the recognition and selectivity of the initially bound substrate and the release of the product formed following chemical transformation. In aqueous solution the stability of the recognition complex is related to hydrogen bonding and Coulombic interactions as well as the geometrical “fit” of the substrate with respect to the receptor polyammonium macrocycle. A feature desirable for catalytic behavior is strong binding of the substrate but relatively weak binding of the product so as to favor dissociation of the resultant complex and release of the macrocycle to continue the catalytic cycle. In order to determine the effect of overall anionic charge and geometry of the substrate on the stability of the complex species formed, and hence its suitability as a possible molecular catalyst,

the interaction of the various protonated forms of the hexaaza macrocycle 3,6,9,17,20,23-hexaazatricyclo[23.3.1.1^{11,15}]triaconta-1(29),11(30),12,14,25,27-hexaene, BMXD (**1**), with mono-, di-, and triphosphosphate anions was investigated. Potentiometric equilibrium methods have been utilized to determine the species present in solution as a function of pH. These results are compared with similar studies involving other hexaaza macrocycles, O-BISDIEN (**2**) and BFBD (**3**). While these macrocycles have the same number of atoms in the main macrocyclic ring, **1** differs from **2** and **3** in not having additional hetero atoms in the ring and having only six basic amino groups as coordinating functions. In addition, the crystal structures of the hexahydrobromide salt of **1**, (H₆BMXD)Br₆·7H₂O (**4**), and the binary complex (H₄BMXD-H₂P₂O₇)Br₂·5.2H₂O (**5**) are presented.

Experimental Section

Materials. The ligand BMXD was prepared as a colorless hexahydrobromide salt according to a published procedure.⁷ GR grade KCl was obtained from EM Chemical Company and CO₂-free Dilut-it ampoules of KOH from J. T. Baker Inc. Reagent grade potassium dihydrogenphosphate and tetrasodium pyrophosphate were purchased from Fisher Scientific Co. and were purified by recrystallization from distilled water. Sodium triphosphosphate (technical grade, 85%) was purchased from Aldrich Chemical Co. and was purified by repeated crystallization from aqueous solution by the addition of methanol.⁸ The KOH solution was standardized by titration against standard potassium acid phthalate using phenolphthalein as indicator and was checked periodically for carbonate content (<2%).⁹

Potentiometric Determinations. Potentiometric measurements were conducted in a jacketed cell thermostated at 25.0 ± 0.1 °C and under an inert atmosphere of purified argon. A Corning Model 350 pH meter fitted with glass and calomel reference electrodes was used. KCl was employed as supporting electrolyte to maintain the ionic strength $\mu = 0.10$ M. The apparatus was calibrated in terms of $-\log[\text{H}^+]$, designated as p[H], by titration of a small quantity of dilute HCl at 0.10 M ionic

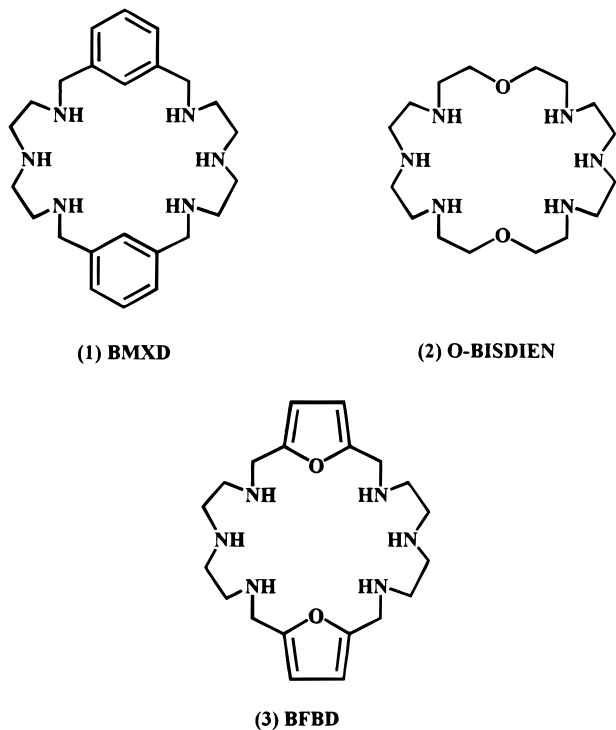
[Ⓞ] Abstract published in *Advance ACS Abstracts*, July 1, 1996.

- (1) Hosseini, M. W.; Lehn, J.-M. *Helv. Chim. Acta* **1987**, *70*, 1312.
- (2) Andrés, A.; Aragón, J.; Bencini, A.; Bianchi, A.; Domenech, A.; Fusi, V.; García-España, E.; Paoletti, P.; Ramírez, J. A. *Inorg. Chem.* **1993**, *32*, 3418.
- (3) Lu, Q.; Motekaitis, R. J.; Reibenspies, J. J.; Martell, A. E. *Inorg. Chem.* **1995**, *34*, 4958.
- (4) Hosseini, M. W.; Lehn, J.-M.; Mertes, M. P. *Helv. Chim. Acta* **1983**, *66*, 2454.
- (5) Hosseini, M. W.; Lehn, J.-M.; Maggiora, L.; Mertes, K. B.; Mertes, M. P. *J. Am. Chem. Soc.* **1987**, *109*, 537.
- (6) Hosseini, M. W.; Lehn, J.-M. *J. Chem. Soc., Chem. Commun.* **1991**, 451.

(7) Menif, R.; Martell, A. E.; Squattrito, P. J.; Clearfield, A. *Inorg. Chem.* **1990**, *29*, 4723.

(8) Watters, J. I.; Loughran, E. D.; Lambert, S. M. *J. Am. Chem. Soc.* **1956**, *78*, 4855.

(9) Martell, A. E.; Motekaitis, R. J. *Determination and Use of Stability Constants*; 2nd ed., VCH Publishers: New York, 1992.



strength and 25.0 °C followed by adjustment of the meter so as to minimize the calculated $p[H]$ vs observed values. The value of $\log K_w$ for the system, defined in terms of $\log([H^+][OH^-])$, was found to be -13.78 at the ionic strength employed¹⁰ and was maintained fixed during refinements.

Acid dissociation constants for the series of phosphate anions were determined under the exact conditions employed in this work and were found to agree well with the literature.¹⁰ Protonation measurements of BMXD and 1:1 ratios of BMXD to each of mono-, di-, and triphosphate anions were obtained at concentrations of approximately 1×10^{-3} M and ionic strength $\mu = 0.10$ M (KCl). Each titration utilized at least 8 points per neutralization of a proton and titrations were repeated until satisfactory agreement was obtained (at least three sets of data were used to calculate the relevant stability constants and their standard deviations). The range of accurate $p[H]$ measurement was considered to be 2–12. Equilibrium constants and species distribution diagrams were calculated using the programs BEST and SPE respectively.⁹

Crystal Structure Determinations. Colorless prisms of $(H_6\text{-BMXD})\text{Br}_6 \cdot 7H_2O$, **4**, were grown by the slow diffusion of acetone into an aqueous solution of the hexahydrobromide salt at 5 °C. Colorless blocks of the binary complex $(H_4\text{BMXD-H}_2\text{P}_2\text{O}_7)\text{Br}_2 \cdot 5.2H_2O$, **5**, were obtained from an aqueous equimolar solution of BMXD.6HBr and $\text{Na}_4\text{P}_2\text{O}_7$, that had been adjusted to $p[H] \sim 3.3$ with dilute HBr, and acetone allowed to diffuse in slowly at room temperature. The binary complex took several weeks to crystallize.

Crystals of **4** and **5** were mounted on glass fibers at room temperature. Preliminary examinations and data collection were performed on a Rigaku AFC5 diffractometer operating in the bisecting mode (oriented graphite monochromator; $\text{MoK}\alpha$ radiation) at 163(2) and 193(2) K for **4** and **5** respectively. Cell parameters were calculated from the least-squares fitting for 25 high-angle reflections ($2\theta > 15^\circ$).

Data was collected for 5.0–50.0° in 2θ for **4** and **5**. Scan width for data collection was 1.54° for **4** and 1.67° for **5** on ω with a variable scan rate between 8 and 16 deg/min. Weak reflections were rescanned (maximum of two rescans) and the counts for each scan were accumulated. Three standards, collected every 97 reflections, showed no significant trends for either **4** or **5**. Background measurements were made by stationary crystal and stationary counter technique at the beginning and the end of each scan for half the total scan time.

Lorentz and polarization corrections were applied to 3603 reflections for **4** and 4982 reflections for **5**. A semiempirical absorption correction was applied.¹¹ The agreement between equivalent reflections for **5** was $R_{int} = 0.0396$; no equivalent reflections were measured for **4**. A total of 3580 and 4854 unique reflections for **4** and **5** respectively were used in further calculations. The structure was solved by direct methods.¹² Examination of intensity distributions uniquely defined the space groups for **4** and **5** to be $Pna2_1$ and $C2/c$, respectively. Full-matrix least-squares anisotropic refinement for all non-hydrogen atoms yielded $R_w(F^2) = 0.128$ and $R(F) = 0.063$ at convergence for **4** and $R_w(F^2) = 0.176$ and $R(F) = 0.076$ at convergence for **5**.¹³ The Flack absolute structure parameter¹⁴ was refined to 0.06(3) for the noncentrosymmetric **4**, which indicated that the correct configuration had been chosen. Hydrogen atoms were placed in idealized positions with isotropic thermal parameters fixed at 0.08 \AA^2 . Neutral atom scattering factors and anomalous scattering factors were taken from ref 24.

The structural analysis of **5** showed slight disorder in the position of one of the two bromide counter ions. The disordered bromide ion was found to exist at a special position in the cell, Br(2), and also to be partially located at the positions defined by Br(3) and Br(3') with populations of 0.35 and 0.15, respectively. Water molecules adjacent to these bromide sites were also found to be only partially occupied and, together with the fully occupied water sites, added up to a total of 5.2 water molecules in the asymmetric unit.

Results and Discussion

Structure of $(H_6\text{BMXD})\text{Br}_6 \cdot 7H_2O$ (4**).** The structure of the hexahydrobromide salt of BMXD was determined by X-ray methods. A summary of the data collection and refinement parameters is given in Table 1. A table of selected bond lengths and angles is given in Table 2.

The structure of **4** is indicated in Figure 1 and consists of the hexaprotonated macrocycle, six bromide counterions, and seven waters of crystallization. The ring containing the nitrogen atoms is approximately planar, but the aromatic rings tilt at an angle of 60° to this plane, one up and one down, such that they remain parallel to each other. The chair conformation of the macrocycle in this case is similar to that found in the crystal structure of the hexahydrobromide salt of the hexaazamacrocycle derived from the condensation of isophthalaldehyde and dipropylentriamine,¹⁵ except in the latter instance the aromatic rings are at an even greater angle (approximately 90°) to the plane defined by the nitrogen atoms. Other reported structures have shown similar macrocycles to adopt boat conformations of the macrocyclic ring.¹⁶ The macrocyclic cavity may be described as an approximate ellipsoid with the major axis being the C(1) to C(18) distance (9.48(2) Å) and the minor axis being the N(2) to N(5) distance (6.35(2) Å).

Two adjacent nitrogen atoms in each diethylene triamine moiety, N(1)–N(2) and N(4)–N(5), face into the macrocyclic cavity and are held in this configuration by hydrogen bonding with an encapsulated bromide ion, Br(1) and Br(2) respectively, while the third nitrogen atom faces outward, N(3) and N(6). Br(1) and Br(2) are the only anions bound close to the center of the macrocycle and interact with it the strongest. Each of

(11) North, A. C.; Phillips, D. C.; Mathews, F. *Acta Crystallogr.* **1968**, A24, 350.

(12) Sheldrick, G. SHELXS-86 Program for Crystal Structure Solution. Institut für Anorganische Chemie der Universität, Tammanstrasse 4, D-3400 Gottingen, Germany, 1986.

(13) Sheldrick, G. SHELXS-93 Program for Crystal Structure Refinement. Institut für Anorganische Chemie der Universität, Tammanstrasse 4, D-3400 Gottingen, Germany, 1993.

(14) Flack, H. D. *Acta Crystallogr.* **1983**, A39, 876. Bernardinelli, G.; Flack, H. D. *Acta Crystallogr.* **1985**, A41, 500.

(15) Llobet, A.; Reibenspies, J.; Martell, A. E. *Inorg. Chem.* **1994**, 33, 5946.

(16) Bencini, A.; Bianchi, A.; Garcia-Espana, E.; Scott, E. C.; Morales, L.; Wang, B.; Deffo, T.; Takusagawa, F.; Mertes, M. P.; Mertes, K. B.; Paoletti, P. *Bioorg. Chem.* **1992**, 20, 8.

(10) Smith, R. M.; Martell, A. E. *NIST Critical Stability Constants Database*, Version 2; NIST: Washington, DC, 1995.

Table 1. Summary of Crystal Data Collection and Refinement Parameters for **4** and **5**

	4	5
empirical formula	C ₂₄ H ₅₈ Br ₆ N ₆ O ₇	C ₂₄ H _{54.4} Br ₂ N ₆ O _{12.2} P ₂
fw	1022.22	844.10
space group	<i>Pna</i> 2 ₁	<i>C2/c</i>
cryst syst	orthorhombic	monoclinic
<i>a</i> , Å	11.597(4)	28.194(6)
<i>b</i> , Å	12.604(4)	13.875(3)
<i>c</i> , Å	27.361(7)	20.811(4)
α , deg	90	90
β , deg	90	113.72(3)
γ , deg	90	90
<i>Z</i>	4	8
<i>V</i> , Å ³	3999(2)	7453(3)
<i>D</i> _{calc} , g/cm ³	1.698	1.504
temp, K	163(2)	193(2)
μ (Mo K α), mm ⁻¹	6.067	2.323
λ , Å	0.71073	0.71073
<i>F</i> (000)	2040	3504
cryst size, mm	0.3 × 0.2 × 0.1	0.4 × 0.3 × 0.1
θ range, deg	2.76 to 25.05	2.08 to 22.52
index ranges (h, k, l)	0 to 13, 0 to 15, 0 to 32	0 to 30, 0 to 14, -22 to 20
no. of reflns colld	3603	4982
max and min transm	0.9999 and 0.5148	0.959 and 0.617
final <i>R</i> indices	<i>R</i> (<i>F</i>) = 0.0625, <i>R</i> _w (<i>F</i> ²) = 0.1283	<i>R</i> (<i>F</i>) = 0.0758, <i>R</i> _w (<i>F</i> ²) = 0.1755
largest diff peak and hole, e Å ⁻³	0.822 and -0.764	0.981 and -0.949

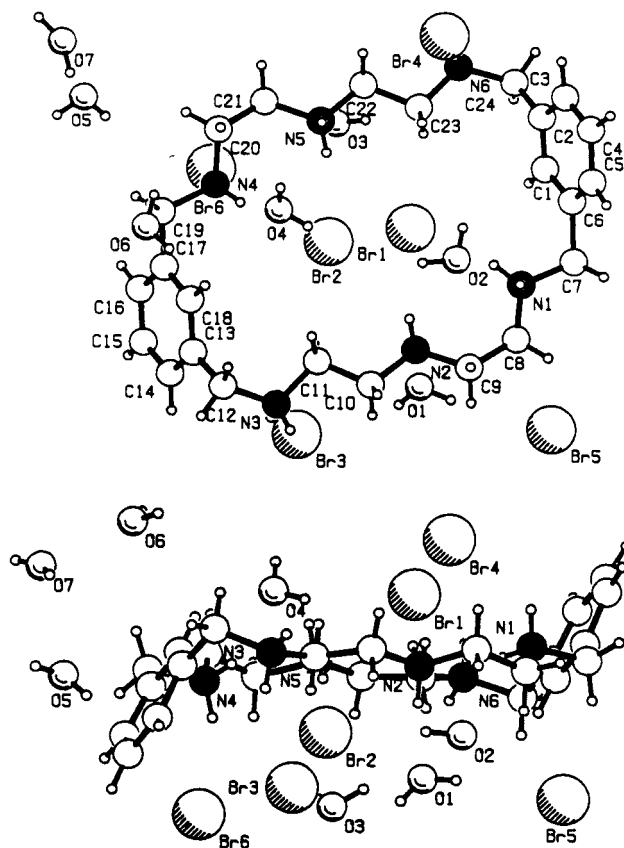
^a $R(F) = \sum |F_o| - |F_c| / \sum |F_o|$. ^b $R_w(F^2) = (\sum w(F_o^2 - F_c^2)^2)^{1/2} \cdot w^{-1} = \sigma^2 F_o^2 + (x(F_o^2 + 2F_c^2)/3)^2 + y(F_o^2 + 2F_c^2)/3$. Key: **4**, $x = 0.0600$, $y = 3.2574$; **5**, $x = 0.0824$, $y = 106.8792$.

Table 2. Selected Bond Lengths (Å) and Angles (deg) for **4** (Standard Deviations in Parentheses)

Br(1)–N(2)	3.41(3)	N(1)–C(7)	1.49(2)
Br(1)–N(1)	3.28(3)	N(2)–C(9)	1.48(4)
Br(1)–N(6')	3.21(2)	N(2)–C(10)	1.52(3)
Br(2)–N(4)	3.35(3)	N(3)–C(12)	1.49(3)
Br(2)–N(3')	3.29(3)	N(3)–C(11)	1.52(3)
Br(2)–N(5)	3.41(2)	N(4)–C(20)	1.50(2)
Br(3)–N(3)	3.29(3)	N(4)–C(19)	1.53(3)
Br(4)–N(6)	3.33(2)	N(5)–C(22)	1.48(3)
Br(5)–N(1')	3.30(2)	N(5)–C(21)	1.55(3)
Br(6)–N(4)	3.28(2)	N(6)–C(23)	1.45(3)
N(1)–C(8)	1.47(2)	N(6)–C(24)	1.51(2)
C(8)–N(1)–C(7)	112.3(14)	C(20)–N(4)–C(19)	114(2)
C(9)–N(2)–C(10)	112(2)	C(22)–N(5)–C(21)	111(2)
C(12)–N(3)–C(11)	114(2)	C(23)–N(6)–C(24)	118(2)

Br(1) and Br(2) forms a hydrogen bond with the two chelating nitrogen atoms of one macrocycle and another nitrogen atom from an adjacent molecule in addition to interacting with the nearby water molecules. Br(1) and Br(2) are displaced from the least-squares plane defined by the nitrogen atoms of the macrocyclic ring (equation of plane: $10.874x - 4.378y + 0.30z = 1.59$) by 1.61(1) and 1.58(1) Å, respectively. The direction of displacement in each case is toward the nitrogen atom of the adjacent macrocycle to which they are hydrogen bonded. The remaining bromide ions each form close contacts with one nitrogen atom and water molecules. The bromide–nitrogen distances in all contacts are typical for hydrogen bonding interactions and range from 3.21 to 3.41 Å with an average of 3.32 Å, Table 2. These distances are comparable to those found in a similar structure¹⁵ although in that case all the bromide ions reside outside of the macrocyclic ring.

The binding of chloride ion to highly protonated polyazamacrocycles probably occurs in solution where chloride is present as part of the supporting electrolyte, but the binding stability constants are usually small enough to be ignored relative to the

**Figure 1.** Diagram of (H₆BMXD)Br₆·7H₂O, **4**, top and side views, respectively, showing the atomic numbering scheme. Hydrogen atoms have been placed in calculated positions.

more strongly bound multidentate anions.¹⁷ The fact that the structure of **4** reveals two bromide ions encapsulated in the macrocyclic ring, whereas the structure of the hexahydrobromide salt of a similar macrocycle¹⁵ does not, demonstrates not a marked difference in affinity for the bromide ion but the subtle difference in crystal packing forces that determine how cations and anions will arrange themselves. The geometry of BMXD is well suited to the binding of anions that provide for multiple electrostatic and hydrogen bonding interactions.

Protonation Constants of BMXD. The ligand protonation constants have been previously determined,⁷ but as different experimental conditions were employed in that work (KNO₃ rather than KCl as supporting electrolyte), the protonation constants were redetermined, Table 3. Comparison of the two sets of results for BMXD indicates good agreement for the mono- through triprotonated stepwise equilibrium constants but those of the tetra- through hexaprotonated constants differ significantly. This would normally be explained in terms of differences in binding constants of the chloride and nitrate anion by the highly charged protonated macrocycle, but, even though chloride and nitrate binding has been observed in other polyamine systems,¹⁷ there seems to be no trend in the differences between the stepwise protonation constants, $\log K^H_i$ ($i = 4, 5, 6$), for both sets of data that would indicate the stronger binding of, say, nitrate ion over chloride ion. The stepwise protonation constants and $\sum \log K^H_i$ for O-BISDIEN and BFBD are included in Table 3 for comparison. The overall basicity ($\sum \log K^H_i$) of BMXD is less than that of O-BISDIEN but greater than that of BFBD. Even though O-BISDIEN contains an aliphatic ether linkage between the diethylenetriamine

(17) Motekaitis, R. J.; Martell, A. E.; Lehn, J.-M.; Watanabe, E. I. *Inorg. Chem.* **1982**, *21*, 4253.

Table 3. Logarithms of the Protonation Constants of BMXD, O-BISDIEN, and BFBD

symbol	equilibrium quotient	log K_i^H			
		BMXD ^a	BMXD ^b	OBISDIEN ^c	BFBD ^d
K_1^H	[HL]/[H][L]	9.51(3)	9.49	9.62	9.44
K_2^H	[H ₂ L]/[H][HL]	8.77(2)	8.73	8.89	8.68
K_3^H	[H ₃ L]/[H][H ₂ L]	7.97(2)	8.03	8.29	7.63
K_4^H	[H ₄ L]/[H][H ₃ L]	7.09(2)	7.29	7.62	6.46
K_5^H	[H ₅ L]/[H][H ₄ L]	3.79(1)	3.64	3.82	3.84
K_6^H	[H ₆ L]/[H][H ₅ L]	3.27(5)	3.45	3.30	3.18
$\Sigma \log K_i^H$		40.40	40.63	41.54	39.23

^a This work, 25.0 °C $\mu = 0.10$ M (KCl) (standard deviations in parentheses). ^b Reference 7, 25.0 °C $\mu = 0.10$ M (KNO₃). ^c Reference 18, 25.0 °C $\mu = 0.10$ (KCl). ^d Reference 3, 25.0 °C $\mu = 0.10$ (KCl).

moieties the electron withdrawing effects of the aromatic rings in BMXD have a greater detrimental effect on the basicity of the adjacent amino nitrogen atoms. The incorporation of an oxygen atom into these aromatic rings, such as the furan moieties of BFBD, increases the electron-withdrawing effect even more and results in a still lower overall basicity than that of BMXD.

Binding of Monophosphate by BMXD. The successive protonation constants of monophosphate were determined in this work and were found to be 11.50(2), 6.76(1), and 1.92(1) at 25.0 °C and $\mu = 0.10$ M (KCl). Because of the high first protonation constant of PO₄³⁻, the dianion, HPO₄²⁻, and the monoanion, H₂PO₄⁻, are the only important species in the practical working p[H] range.

Examination of the curve obtained when BMXD was titrated in the presence of one equivalent of monophosphate anion indicated the existence of BMXD–phosphate complex species in the region from p[H] \sim 2–6. The stability constants for these species are given in Table 4. The values obtained for the association constants of the complex species that form between BMXD and monophosphate are remarkably similar to those of the same species obtained with the ligand O-BISDIEN.^{18,19} In those studies, however, other binary species were also detected that were not present in the BMXD–phosphate system. In the present system the interaction of BMXD with the monophosphate ion is appreciable only up to p[H] \sim 6.

When the equilibria are expressed in terms of the association of the protonated macrocycle with the hydrogenphosphate anion, it is clear that the value of log K increases with the increasing degree of protonation of the macrocycle. This can be readily understood in terms of the greater Coulombic attraction that exists between the anion and the macrocycle as the degree of protonation increases as well as the increase in hydrogen-bonding interactions that are possible. At lower p[H] the binary species H₆BmPh³⁺ and H₇BmPh⁴⁺ probably arise through interaction of the dihydrogenphosphate anion with the appropriate protonated macrocycle. Equilibrium constants for these interactions are included in Table 4.

Structure of (H₄BMXD–H₂P₂O₇)Br₂·5.2H₂O (5). The structure of the binary complex **5** was determined by X-ray diffraction techniques. A summary of the data collection and refinement parameters is included in Table 1. Selected bond lengths and angles are given in Table 5.

Although the possibility exists for the pyrophosphate (diphosphate) anion to bind facially to the protonated macrocycle this is not seen in this instance. The tetraprotonated macrocycle

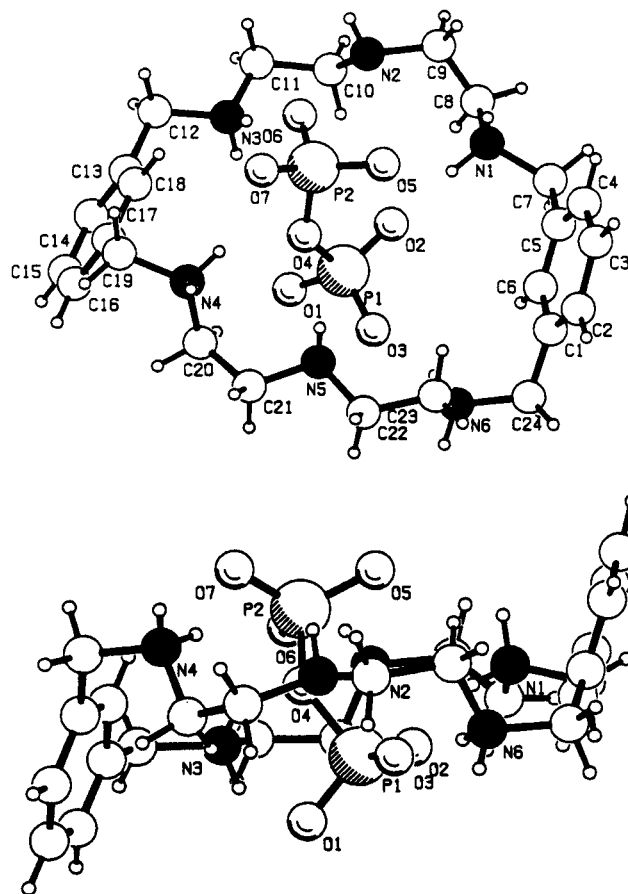


Figure 2. Top and side views, respectively, of the binary complex cation (H₄BMX)–H₂P₂O₇]²⁺, **5**, showing the atomic numbering scheme. Hydrogen atoms have been placed in calculated positions.

binds the dihydrogen pyrophosphate ion inside the macrocyclic cavity, as depicted in Figure 2. Using the ellipsoid description for the dimensions of the macrocyclic ring, the inclusion of the pyrophosphate anion causes a contraction of the major axis from 9.48(2) to 8.48(2) Å when compared to **4** and an expansion of the minor axis from 6.35(2) to 7.65(3) Å. These less elliptical dimensions result in the puckering of the ring into a twisted chair type conformation.

Each end of the pyrophosphate anion is hydrogen bonded to the nitrogen atoms of a *m*-xylyldiamine moiety through two of its oxygen atoms while the third oxygen atom, bearing a proton, points away from the cavity and is hydrogen bonded to a nitrogen atom of an adjacent molecule. The pyrophosphate oxygen–nitrogen bond distances range from 2.60 to 2.75 Å with an average of 2.67 Å and are comparable to similar pyrophosphate O···N distances.^{20,21} The non-protonated secondary amines of the diethylenetriamine bridge also make close contacts with an oxygen atom of the pyrophosphate anion, N(2)–O(6) and N(5)–O(3), 2.68 and 2.72 Å respectively. Their proximity to the anion is noteworthy as it is these central amino nitrogen atoms of O-BISDIEN that are responsible for the nucleophilic attack on the bound polyphosphate substrate that leads to the catalytic hydrolysis of ATP in model systems.²²

The arrangement of the anion within the macrocyclic cavity is such that it can be considered almost axial to the macrocyclic “plane” rather than coplanar with it. The mode of binding of

(18) Motekaitis, R. J.; Martell, A. E. *Inorg. Chem.* **1992**, *31*, 5534.

(19) Motekaitis, R. J.; Martell, A. E. *Inorg. Chem.* **1994**, *33*, 1032.

(20) Bartoszak, E.; Jaskólski, M. *Acta Crystallogr.* **1990**, *C46*, 2158.

(21) Labadi, I.; Sillanpää, R.; Lönnberg, H. *J. Chem. Soc., Dalton Trans.* **1992**, 765.

(22) Hosseini, M. W.; Lehn, J.-M.; Jones, K. C.; Plute, K. E.; Mertes, K. B.; Mertes, M. P. *J. Am. Chem. Soc.* **1989**, *111*, 6330.

Table 4. Overall Formation Constants (β) and Stepwise Association Constants (K) for the BMXD–Monophosphate System (Bm = BMXD; Ph = PO₄³⁻)

stoichiometry			log β^a	equilibrium quotient, ^b K	log K	principal equilibrium, ^b K'	log K'
Bm	Ph	H					
1	1	5	47.72(8)	[H ₅ BmPh]/[H ₄ Bm][HPh]	2.87	[H ₅ BmPh]/[H ₄ Bm][HPh]	2.87
1	1	6	54.10(7)	[H ₆ BmPh]/[H ₅ Bm][HPh]	5.47	[H ₆ BmPh]/[H ₄ Bm][H ₂ Ph]	2.49
1	1	7	59.26(2)	[H ₇ BmPh]/[H ₆ Bm][HPh]	7.36	[H ₇ BmPh]/[H ₅ Bm][H ₂ Ph]	3.86

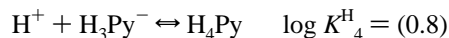
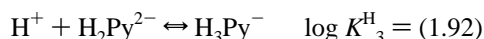
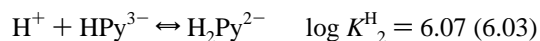
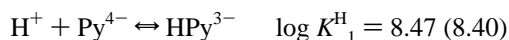
^a $\mu = 0.10$ M (KCl), 25.0 °C (standard deviations in parentheses). ^b Charges have been omitted for clarity.

Table 5. Selected Bond Lengths (Å) and Angles (deg) for **5** (Standard Deviations in Parentheses)

N(1)–O(2)	2.597(8)	P(1)–O(2)	1.503(6)
N(3)–O(6)	2.708(9)	P(1)–O(3)	1.509(6)
N(2)–O(6)	2.683(8)	P(1)–O(1)	1.512(7)
N(2)–O(1')	2.610(10)	P(1)–O(4)	1.622(6)
N(6)–O(3)	2.636(9)	P(2)–O(6)	1.511(6)
N(4)–O(7)	2.753(9)	P(2)–O(7)	1.515(6)
N(4)–O(5')	2.679(8)	P(2)–O(5)	1.516(6)
N(5)–O(3)	2.719(8)	P(2)–O(4)	1.604(6)
N(5)–O(7')	2.655(10)		
O(2)–P(1)–O(3)	115.9(4)	O(6)–P(2)–O(5)	112.7(3)
O(2)–P(1)–O(1)	112.6(4)	O(7)–P(2)–O(5)	112.7(3)
O(3)–P(1)–O(1)	110.7(4)	O(6)–P(2)–O(4)	107.2(3)
O(2)–P(1)–O(4)	109.1(3)	O(7)–P(2)–O(4)	101.6(3)
O(3)–P(1)–O(4)	103.3(3)	O(5)–P(2)–O(4)	108.1(4)
O(1)–P(1)–O(4)	104.3(3)	P(2)–O(4)–P(1)	132.6(4)
O(6)–P(2)–O(7)	113.6(3)		

the pyrophosphate anion to BMXD, with each “end” of the anion hydrogen bonded to a *m*-xylyl diamine moiety, suggests that it tends to align itself along the major axis of the elliptical macrocyclic ring and not the minor axis. This differs with the postulated preferred orientation of nucleotides with respect to macrocycles of this type.¹⁶ The inclusion of the pyrophosphate anion wholly within the macrocyclic cavity is in contrast with the structure of the BFBD–pyrophosphate binary complex where the anion extended outside the macrocycle and was engaged in intermolecular hydrogen bonding with the neighboring pyrophosphate.³

Binding of Diphosphate Anion by BMXD. The two most basic protonation constants of pyrophosphoric acid (H₄Py) were determined under the conditions employed in this work and were found to agree closely with the literature values (given in parentheses below).¹⁰ The third and fourth protonation constants were not calculated but were taken directly from the literature.¹⁰



When BMXD was titrated in the presence of 1 equiv of sodium pyrophosphate a new titration curve was obtained which, because of the large deviations between calculated and observed p[H] values in certain regions, indicated the presence of complex binary species. The stability constant results are given in Table 6. Comparison of the stability constants of the complex species found with BMXD to the same species formed with either O-BISDIEN or BFBD shows that BMXD forms slightly more stable complexes. Both O-BISDIEN²³ and BFBD³ are able to form further complex binary species with the pyrophosphate

anion in addition to those that form with BMXD, but the stability constants of these additional species are progressively smaller.

When the stability constants are expressed in terms of the binding of the pyrophosphate anion to the various protonated forms of BMXD, log K , it is evident that the magnitude of the association constant increases rapidly with the degree of protonation of the macrocycle. This is due to both the increase in Coulombic attraction between the reacting species and the formation of extensive hydrogen bonding. It is not surprising therefore that the largest association constant is found for the interaction of the fully protonated macrocycle with the fully deprotonated anion, (H₆Bm)(Py).

It cannot be stated with certainty which species actually come together to form the binary complexes but on the basis of titrations of the individual constituents, reasonable guesses of the principal equilibria can be made. The variation in these association constants, log K' , can be explained using the same arguments of electrostatic attraction and hydrogen bonding interactions. Using these arguments, and considering the principal equilibria, one would expect the association stability constant of H₅BmPy⁺ to be greater than that of H₆BmPy²⁺ due to the higher negative charge of HPy³⁻ when compared to H₂Py²⁻, while the degree of macrocyclic protonation remains the same. This is however not the case and the magnitude of log K' for H₅BmPy⁺ and H₆BmPy²⁺ do not differ greatly, 5.25 and 5.58 respectively. One possible explanation for this can be derived from the crystal structure determination of (H₄-BMXD-H₂P₂O₇)Br₂·5.2H₂O. Figure 2 shows that the dihydrogen pyrophosphate anion is bound to the macrocycle by way of hydrogen bonds between two oxygen atoms from each end of the anion and the four protonated secondary nitrogen atoms leaving the protonated oxygen on each end of the pyrophosphate anion pointing away from the macrocycle and engaging in its own hydrogen-bonding interaction with a nitrogen atom of a neighboring molecule. In solution, deprotonation of one of these terminal oxygen atoms likely has little effect on the interaction between the remaining pyrophosphate oxygen atoms and the macrocycle, leading to only a small change in the magnitude of the binding constants.

The ion selectivity that BMXD displays is best exemplified in Figure 3 which shows the distribution of species in a solution containing BMXD, monophosphate, and pyrophosphate each at 1.0 × 10⁻³ M concentration. Only binary species are shown and it is clearly evident that the species containing pyrophosphate ions bound to the macrocycle predominate over those containing monophosphate ions. In the presence of pyrophosphate, monophosphate binary species account for less than 5% of the total amount of binary species in the p[H] range 2–8. All binary interactions cease above p[H] = 9, after which the constituents coexist independently of each other.

Binding of Tripolyphosphate Anion by BMXD. The first and second protonation constants of tripolyphosphate anion (Tr⁵⁻) were found to be 8.07 and 5.53 at 25.0 °C and $\mu = 0.10$ M (KCl). The values given in the literature are 7.98, 5.49, 2.0,

(23) Jurek, P. E.; Martell, A. E.; Motekaitis, R. J.; Hancock, R. D. *Inorg. Chem.* **1995**, *34*, 1823.

(24) *International Tables for X-ray Crystallography*; D. Riedel: Dordrecht, The Netherlands, 1985; Vol. C.

Table 6. Overall Formation Constants (β) (BMXD–Pyrophosphate) and Stepwise Association Constants (K) for the Interaction of Pyrophosphate with L (L = BMXD, O-BISDIEN, or BFBD; Py = $\text{P}_2\text{O}_7^{4-}$; $\mu = 0.10$ M (KCl), 25.0 °C)

stoichiometry			$\log \beta^a$	equilibrium quotient, ^d K	$\log K$	principal equilibrium, ^d K'	$\log K'$		
L	Py	H					BMXD	O-BISDIEN ^b	BFBD ^c
1	1	1				[HLPy]/[HL][Py]	2.07		2.20
1	1	2				[H ₂ LPy]/[H ₂ L][Py]	2.41		2.61
1	1	3				[H ₃ LPy]/[H ₃ L][HPy]	3.31		2.45
1	1	4	39.07(5)	[H ₄ LPy]/[H ₄ L][Py]	5.73	[H ₄ LPy]/[H ₃ L][HPy]	4.35	4.44	3.61
1	1	5	47.07(5)	[H ₅ LPy]/[H ₅ L][Py]	9.94	[H ₅ LPy]/[H ₄ L][HPy]	5.25	4.74	4.82
1	1	6	53.47(6)	[H ₆ LPy]/[H ₆ L][Py]	13.07	[H ₆ LPy]/[H ₄ L][H ₂ Py]	5.58	5.36	4.93
1	1	7	58.04(5)	[H ₇ LPy]/[H ₆ L][HPy]	6.14	[H ₇ LPy]/[H ₅ L][H ₂ Py]	6.36	6.25	5.57
1	1	8				[H ₈ LPy]/[H ₆ L][H ₂ Py]	4.86		4.53

^a This work (standard deviations in parentheses). ^b Reference 23. ^c Reference 3. ^d Charges have been omitted for clarity.

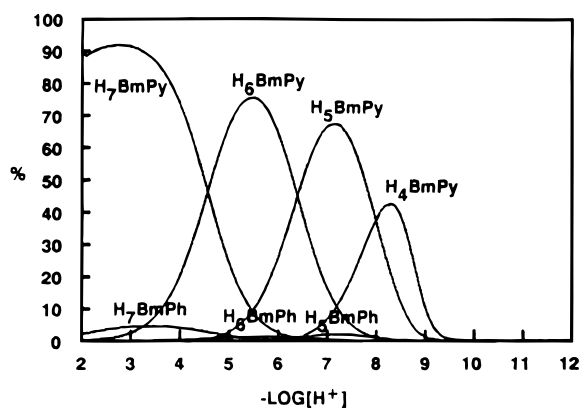


Figure 3. Species distribution diagram showing the species formed as a function of p[H] when 1.0×10^{-3} M BMXD·6HBr, 1.0×10^{-3} M PO_4^{3-} , and 1.0×10^{-3} M $\text{P}_2\text{O}_7^{4-}$ are equilibrated at 25.0 °C and $\mu = 0.10$ M (KCl). Only the binary species are shown.

1.2, and 0.7.¹⁰ Due to the low value of the third protonation constant of tripolyphosphate the only species of importance in the working p[H] range are the $\text{H}_2\text{P}_3\text{O}_{10}^{3-}$, $\text{HP}_3\text{O}_{10}^{4-}$, and $\text{P}_3\text{O}_{10}^{5-}$ anions.

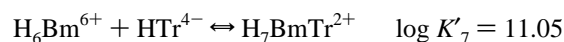
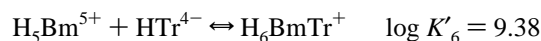
The results of titration of BMXD with tripolyphosphate anion are given in Table 7. The calculations revealed that all complex species of the series $\text{H}_i\text{BmTr}^{i-5}$ ($i = 1-8$) were present with the exception of $i = 2$. Repeated manipulation of the refinement process, e.g. forcing the existence of $\text{H}_2\text{BmTr}^{3-}$ and/or removal of other species, continued to produce this same anomaly. The reason why there exists a jump in the sequence of complex species is unknown.

The large values of the association constants, $\log K$, when compared to those for the diphosphate and monophosphate binary species, indicate the strength of the interaction between protonated BMXD and the tripolyphosphate anion. The \log association constants, $\log K$, for the species HBmTr^{4-} through $\text{H}_6\text{BmTr}^{+}$ increase with increasing degree of protonation of the hexaazamacrocycle as is expected due to the resulting increase in electrostatic attraction and hydrogen-bonding interactions. The strongest interaction occurs between the hexaprotonated macrocycle and the tripolyphosphate anion. Then, as further protons are added to the anion the association constants decrease. The principal equilibria, $\log K'$, express the association of the likely (predominant) species in solution at the p[H] at which binary species reach their maximum concentration. The magnitude of these constants increase in the same order but the differences between successive species is smaller. The most stable complex when considering these equilibria is $\text{H}_7\text{BmTr}^{7+}$. The decline in association constant from 8.79 to 7.56 as the number of protons is increased, $\text{H}_7\text{BmTr}^{2+}$ to $\text{H}_8\text{BmTr}^{3+}$, may be a consequence of an unfavorable conformational change occurring in the macrocycle. As the crystal structure of **4** shows, the hexaprotonated macrocycle tends toward planarity and possibly

does not accommodate tripolyphosphate anion as well in this conformation. It is also pointed out, however, that while the Coulombic attraction goes up, the addition of a hydrogen ion decreases the number of strong hydrogen bonds that can form. A similar effect is seen in the complexes formed between pyrophosphate anion and protonated forms of O-BISDIEN and BFBD (Table 6).

Figure 4 shows the species distribution diagram for an equimolar mixture of BMXD–pyrophosphate–tripolyphosphate, each at a concentration of 1.0×10^{-3} M. The protonated ligand displays a higher affinity for tripolyphosphate than pyrophosphate anion over the whole p[H] range through which such binary interactions are important. The degree of selectivity of tripolyphosphate over pyrophosphate is not as great as that of pyrophosphate over monophosphate (Figure 3) as seen by the larger percentage of BMXD–pyrophosphate species that are present in Figure 4 compared to the percentage of BMXD–orthophosphate species present in Figure 3. At lower p[H] (<6) the tripolyphosphate anion can interact with the polyprotonated macrocycle to a greater extent due to its increased size, which may be important if the macrocycle extends to planarity upon full protonation, and also its greater number of oxygen atoms which are available for hydrogen bonding. Around p[H] 7–9, the differences between the pyrophosphate and tripolyphosphate anion become less important as far as binary complexation is concerned since the partially protonated macrocycle, tetraprotonated for example, can equally accommodate either anion, possibly in very similar coordination modes.

Unfortunately no anion binding studies of hexaazamacrocycles with tripolyphosphate anions have been reported prior to this although analogous work with O-BISDIEN and the nucleotide triphosphate ATP has been described.¹ In that work \log association constants between the tetra-, penta-, and hexaprotonated O-BISDIEN and ATP were found to be 4.80, 8.15, and 11.00 respectively. Since ATP corresponds to monoprotonated tripolyphosphate these values can be compared to those obtained in the BMXD–tripolyphosphate system when the following equilibria are evaluated:



The stability constant for the complexation of the tetraprotonated macrocycle with the tetra-anionic tripolyphosphate is nearly 2 orders of magnitude greater for BMXD than for O-BISDIEN. Interestingly, the association constant for the interaction of H_5Bm^{5+} and the tetraanionic tripolyphosphate is a factor of 17 greater than that of O-BISDIEN whereas the hexaprotonated macrocycle–tripolyphosphate association con-

Table 7. Overall Formation Constants (β) and Stepwise Association Constants (K) for the BMXD–Triphosphate System (Bm = BMXD; Tr = $P_3O_{10}^{5-}$)

stoichiometry			log β^a	equilibrium quotient, ^b K	log K	principal equilibrium, ^b K'	log K'
Bm	Tr	H					
1	1	1	13.02(2)	[HBmTr]/[HBm][Tr]	3.51	[HBmTr]/[HBm][Tr]	3.51
1	1	3	30.96(2)	[H ₃ BmTr]/[H ₃ Bm][Tr]	4.71	[H ₃ BmTr]/[H ₂ Bm][HTr]	4.61
1	1	4	39.81(2)	[H ₄ BmTr]/[H ₄ Bm][Tr]	6.47	[H ₄ BmTr]/[H ₃ Bm][HTr]	5.49
1	1	5	47.98(1)	[H ₅ BmTr]/[H ₅ Bm][Tr]	10.85	[H ₅ BmTr]/[H ₄ Bm][HTr]	6.56
1	1	6	54.59(1)	[H ₆ BmTr]/[H ₆ Bm][Tr]	14.19	[H ₆ BmTr]/[H ₄ Bm][H ₂ Tr]	7.64
1	1	7	59.53(1)	[H ₇ BmTr]/[H ₆ Bm][HTr]	11.06	[H ₇ BmTr]/[H ₅ Bm][H ₂ Tr]	8.79
1	1	8	61.57(7)	[H ₈ BmTr]/[H ₆ Bm][H ₂ Tr]	7.57	[H ₈ BmTr]/[H ₆ Bm][H ₂ Tr]	7.56

^a $\mu = 0.10$ M (KCl), 25.0 °C (standard deviations in parentheses). ^b Charges have been omitted for clarity.

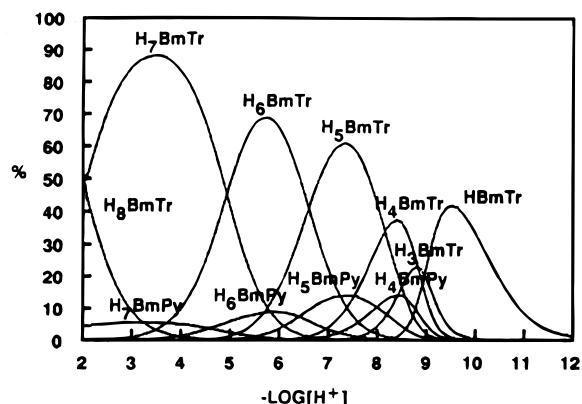


Figure 4. Species distribution diagram showing the species formed as a function of p[H] when 1.0×10^{-3} M BMXD·6HBr, 1.0×10^{-3} M $P_2O_7^{4-}$, and 1.0×10^{-3} M $P_3O_{10}^{5-}$ are equilibrated at 25.0 °C and $\mu = 0.10$ M (KCl). Only the binary species are shown.

stants are almost identical. These differences in binding strength of the anions, especially in the case of the tetraprotonated macrocycle, may have implications toward the rates of ATP binding and hydrolysis, although such a correlation is not necessarily expected.¹⁶ Parallel studies with BMXD and ATP are being undertaken in this laboratory.

Conclusion

This investigation has shown that both the number of complex species formed and the strength of interaction between the protonated hexaazamacrocycle BMXD and inorganic phosphate anion increases in the order monophosphate < diphosphate <

triphosphate. This is an effect of not only the increase in negative charge of the anionic substrate and hence the increase in Coulombic attraction for the protonated macrocycle, but also the increase in number of oxygen atoms in the substrate that are able to engage in hydrogen bonding interactions. The effect however is not unlimited in the sense that further increasing the number of condensed phosphates would not be expected to lead to more stable complexes since the macrocycle is only of finite size. Geometrical compatibility of substrate and ligand is therefore important. It is noteworthy that the pyrophosphate anion is almost axial to the macrocyclic “plane” rather than coplanar with it, as is the orientation of the nucleotides with macrocycles of this type.

The marked increase in stability of triphosphate anion binding over both di- and monophosphate binding is probably attributable to the better ability of triphosphate to span the length and breadth of protonated BMXD and therefore take maximum advantage of its many polyammonium sites. The X-ray crystal structure determination of the pyrophosphate–BMXD binary complex demonstrated the ability of the macrocycle to accommodate anions of this type.

Acknowledgment. This work was supported by the Robert A. Welch Foundation.

Supporting Information Available: Atomic coordinates with isotropic displacement parameters for **4** and **5**, Tables SI and SII, respectively, anisotropic displacement parameters, Tables SIII and SIV, and hydrogen atom coordinates, Tables SV and SVI (14 pages). Ordering information is given on any current masthead page.

IC9513090